electronics

Article

A Dimension Estimation Method for Rigid and Flexible Planar Antennas Based on Characteristic Mode Analysis

Bashar Bahaa Qas Elias [1,2,*], Azremi Abdullah Al-Hadi [1], Prayoot Akkaraekthalin [3] and Ping Jack Soh [4]

[1] Advanced Communication Engineering (ACE) CoE, Faculty of Electronic Engineering Technology, Pauh Putra Campus, Universiti Malaysia Perlis (UniMAP), Arau 02600, Perlis, Malaysia
[2] Department of Communications Technology Engineering, College of Information Technology, Imam Ja'afar Al-Sadiq University, Baghdad 10052, Iraq
[3] Department of Electrical and Computer Engineering, Faculty of Engineering, King Mongkut's University of Technology North Bangkok (KMUTNB), 1518 Pracharat 1 Rd., Wongsawang, Bangsue, Bangkok 10800, Thailand
[4] Centre for Wireless Communications (CWC), University of Oulu, P.O. Box 4500, 90014 Oulu, Finland
* Correspondence: bashar.bahaa@sadiq.edu.iq

Abstract: An empirical method for simplified dimension estimation of patch antennas is proposed in this work based on characteristic mode analysis (CMA). This method involves generating formulae to calculate substrate-independent antenna patch widths produced from the antenna's characteristic angle. This enables the definition of a relationship between the characteristic angle and the natural resonant frequency of an antenna structure, bridging the changes of resonant frequencies contributed by possible variation in substrate properties. From here, the end 'calibrated' results can be used to generate specific formulae for each antenna to determine the width of the patch at different operating frequencies, making it time- and resource-efficient. This method was validated using conventional and slotted antennas designed using different substrates, both rigid (RO4003C, Rogers RT/Duroid 5880) and conventional (felt, denim fabric). Measurement results obtained were in satisfactory agreement with simulated results, even without considering the substrates and excitations. Finally, this method was also applied in designing dual-band antennas using flexible materials for wearable applications, indicating good agreement with experimental results.

Keywords: patch width; CMA; substrate material; resonant frequency

Citation: Qas Elias, B.B.; Al-Hadi, A.A.; Akkaraekthalin, P.; Soh, P.J. A Dimension Estimation Method for Rigid and Flexible Planar Antennas Based on Characteristic Mode Analysis. *Electronics* **2022**, *11*, 3585. https://doi.org/10.3390/electronics11213585

Academic Editors: Emanuele Cardillo and Changzhi Li

Received: 15 October 2022
Accepted: 1 November 2022
Published: 2 November 2022

1. Introduction

In recent years, flexible electronic devices have become especially important to cater to various wireless communication applications, such as the internet of things (IoT), emergency services, medical and military [1,2]. Wearable antennas are typically implemented to support the wireless communication capability in such electronic devices. They are designed using flexible materials to ease their integration with clothing when placed on various body locations, such as on the chest, wrist, head, etc. In the past decade, flexible antennas have been designed using different materials including electro-textiles, due to their ease of integration into clothing. These wearable antennas are applied for remote sensing and monitoring of patients with diabetes [3,4], and for monitoring the heart rate [5] in an indoor environment. Furthermore, flexible materials, such as textiles, are low in dielectric constant, which potentially increases antenna bandwidth and reduces the surface wave losses [6].

The theory of characteristic modes (TCM) was first proposed in [7] and refined in [8,9]. Characteristic modes represent a set of orthogonal real currents on the surface of a conducting body. It does not require excitation sources when determining the electromagnetic properties of the structure [10]. This makes it an efficient basis for antenna design, due to its capability in providing direct insights into the antenna's radiating phenomena, allowing

a more systematic design process in place of a tedious optimization approach. Moreover, the insights provided by CMA aid in locating the placement of excitation on any arbitrary antenna and/or on a platform [11] without readily available closed formulation for analyses. TCM provides a natural and systematic method for designing Multiple-Input Multiple-Output (MIMO) antennas with high efficiency [12]. Moreover, recent topics in CMA include a focus on investigating the metasurface structures to improve antenna performance [13,14]. CMA can also be used to improve impedance bandwidth by combining dominant modes operating over the necessary band [15]. In addition to these, the CMA technique has also been applied in optimizing the radiation pattern of antennas [16] and in presenting the systematic procedures for designing platform-integrated antenna [17].

The bandwidth of an antenna can be efficiently estimated by solving only the equivalent eigenmodes. This produces a general electromagnetic solution for the structure, as the results of the analysis are independent of excitation [18]. Using a moment method formulation and the discretized impedance matrix, one can determine the characteristic modes of any perfectly conducting structure, and this feature is what makes this analysis method so attractive [19]. For the computation of patch dimensions, the antenna designer needs practical and accurate formulae. There are several formulae [20–28] in the literature for determining the physical dimensions of the patch, which vary in accuracy and computational effort, as described in the following subsections.

This paper proposes a method determining the dimensions, and predicting the resonant frequencies of planar antennas with different degrees of structural complexity, stemming from the initial work in [29]. The created formula is applied to optimizing radiator dimensions of a dual-band slotted antenna at various stages. Most importantly, an investigation into the accuracy of the proposed method, and its fundamental limitations in estimating the patch dimensions and resonant frequency, is performed. This method contributes to time and effort reduction, due to its ability in predicting resonant frequencies of different antenna topologies and substrate materials.

1.1. Classical Method

Microstrip antennas (MSAs), consisting of a patch, substrate and ground layer, are usually studied using two dielectric media: (i) air over the patch, and (ii) the dielectric substrate underneath. Radiation leads to the fringing fields at the edges. The length of the radiation patch on either side of the patch is then effectively increased by a length commonly described as ΔL. The electric length (*Leff*) of the patch is, therefore, $2\Delta L$ more than its physical length (L). The empirical formula in [20] shows that ΔL can be determined based on the width (W) of the patch, substrate thickness (h) and its effective dielectric constant ($\varepsilon reff$).

1.2. Equivalent Design Concept

A new method in estimating the physical length of a rectangular MSA was proposed in [21,22]. The physical length extension (d) of the patch is directly proportional to the thickness (h) of the substrate, whereas the electrical length (Le) of the patch is inversely proportional to its width (W). The proportionality constant (β) of the height of substrate to guided wavelength is, then, independent of the resonant frequency (fr), thickness, and dielectric constant (εr) of the substrate [23]. This allows new design parameters to be obtained by appropriately scaling an existing design previously optimized for another set of materials. Moreover, the two designs are equivalent if they result in the same resonant frequency, as follows:

$$d \propto \frac{h \times L_e}{W} \tag{1}$$

Or

$$d = \beta \frac{h \times L_e}{W} \tag{2}$$

Hence

$$\frac{d}{h} \times \frac{W}{L_e} = \beta \tag{3}$$

For a rectangular patch, the value of β is unity.

The new approach enables the calculation of the physical length of the patch (Lp), as follows:

$$L_p = (1 - 2\beta H)L_e \tag{4}$$

$$H = \left[\frac{1 - \frac{L_p}{L_e}}{2\beta}\right] \tag{5}$$

Calculations were performed to verify the proposed procedure, as follows:

i. First, the dielectric constant εr was varied from 1 to 10.
ii. For each value of εr, values of β were determined between 1 to 60 GHz. To do so, 15 values of resonant frequency were considered from 1 GHz to 10 GHz in steps of 1 GHz, whereas resonant frequencies of 20, 30, 40, 50 and 60 GHz were simulated. A total of 450 combinations of β were calculated at different frequencies, dielectric constants, and antenna substrate thicknesses.
iii. Three values of the normalized substrate thicknesses (H) were considered: H = 0.005, 0.01 and 0.015. Parameter $H$was calculated as: $H = h/\lambda g$, where λg was the guided wavelength for specific dielectric permittivity.

The value of β was kept constant (unity) in all cases.

1.3. Patch Dimensions for Thin and Thick Substrates

The work in [24] proposes a new closed formula for calculating the patch dimensions of electrically thick and thin rectangular microstrip antennas (RMSAs). They are obtained using a curve fitting technique (CFT), which is useful for computer-aided design of microstrip antennas. A rectangular patch was considered, with a width, W, and length L placed over a ground plane with a substrate of thickness and relative dielectric constant, as shown in Figure 1. To obtain the proper patch dimensions, many experiments were performed to derive the following equation with satisfactory results depending on the chosen h, εr and fr:

$$\text{Patch dimension}(w \text{ or } L) = \alpha_1 \lambda_g \left(h/\lambda_g\right)^{\alpha_2} + \alpha_3 \lambda_d \left(h/\lambda_g\right)^{\alpha_4} + \alpha_5 \lambda_o \tag{6}$$

where λg is the guided wavelength in the dielectric substrate, λo is the free-space wavelength, and the unknown coefficients, α_1, α_2, α_3, α_4, and α_5, are determined by the CFT for electrically thin and thick RMSAs. This approach enables antenna designers to use a single model to estimate both patch width and length, thus, simplifying the procedure in two main steps. The first is the selection of a suitable dielectric substrate material, followed by determining the patch dimensions W and L. Finally, the unknown coefficients of the model are determined using CFT. The results calculated by applying the formulae proposed in Equation (6) were better than those expected in prior studies. The good agreement between measured and estimated patch-dimension values confirmed the validity of the formulae proposed in this study. These formulae enable designers to use a single model for both patch width and length and, thus, simplifying the design. The sum of the absolute errors between the theoretical and experimental results using this method was 0.143.

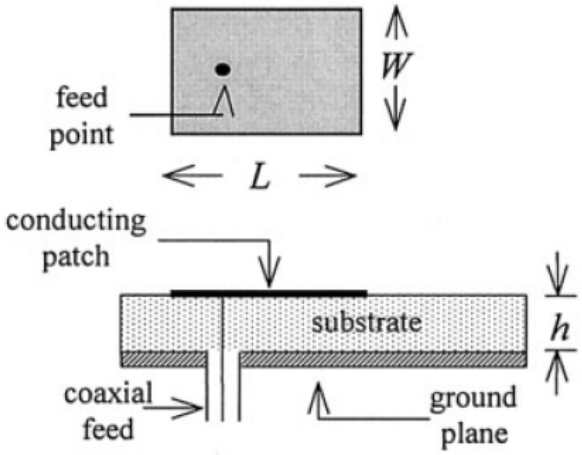

Figure 1. RMSA structure [24].

2. Proposed Method Based on CMA

It is apparent that all the techniques presented in the literature to estimate the dimensions of rectangular MSAs are based on three parameters: thickness, dielectric constant, and resonant frequency. For the same purpose, CMA can be used to derive the design equations. The proposed method in this research involves determining the patch width generated using CMA (WCA) and its relationship between the variables at different resonant frequencies in several steps. This facilitates the estimation of the width of the planar radiator using only CMA without considering the effects of substrate and excitation. To validate this method, four different substrates with varying dielectric permittivity and thicknesses were chosen, as summarized in Table 1.

Table 1. Characteristic of Substrate Materials.

Substrate	Dielectric Constant (εr)	Loss Tangent (tanδ)	Thickness (mm)
Felt	1.3	0.044	3
RO4003C	3.4	0.002	0.085
Denim	1.7	0.085	1
Rogers RT/Duroid 5880	2.2	0.0009	0.508

The formulation process of this method was performed as follows:

i. A simple square patch was modeled without substrate and excitation.
ii. The characteristic angle (CA) resulting from the dimensions of the radiator was analyzed in terms of resonant frequency. If the resulting CA was close to 180°, the patch width was adopted, and this process was repeated for other resonant frequencies. The use of CA simplified the iteration process and reduced the number of cycles to achieve optimal performance.
iii. The full antenna structure (with substrate, ground, and excitation) was then designed and analyzed using MoM. The widths of the antenna producing different resonant frequencies were recorded.

Upon obtaining all patch dimensions from both CMA and MoM methods, relations between dimensions and all resonant frequencies were determined in the form of equations. The final equation was generated, which varied for each substrate material.

These steps generated CMA-based design equations to calculate patch dimensions, as summarized in Figure 2. To properly validate the proposed procedure, a large number of calculations were performed on conventional and slotted antennas designed on different substrates to operate at different resonant frequencies.

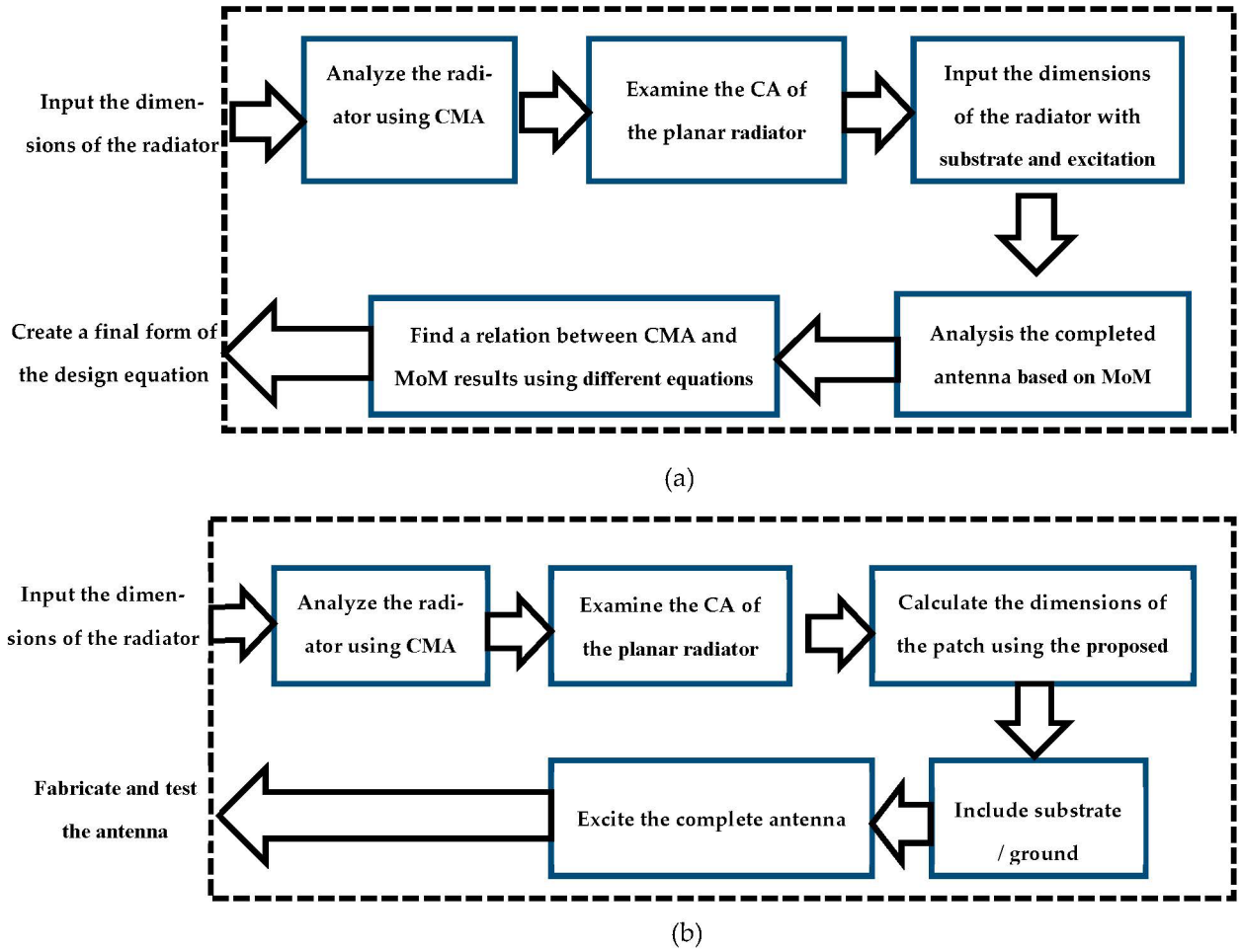

Figure 2. (**a**) Generation of the formula, and (**b**) design procedure using the proposed formula.

2.1. Conventional Antenna

A square microstrip patch antenna is defined as the conventional antenna. First, its patch width and length were calculated using CMA without the substrate and excitation, followed by the width and length calculations of the patch using MoM (including the substrate and excitation). The CA parameter was used, as illustrated in Figure 3. Mode 1 was observed to be the dominant mode, as seen in its close-to-180° value for different operating frequencies.

The equations to perform these estimations were generated as follows:

i. First, the physical width of the radiator patch, *WCA*, was calculated using the CMA method without substrate and excitation. This value was then subtracted from the width value of the patch, *WM-S*. This value was calculated using MoM (to include substrate and excitation) and to result in a new parameter, ΔW, as follows:

$$\Delta W = WCA - WM\text{-}S \tag{7}$$

ii. The average ratio between the patch width produced by a MoM to the difference between the width values produced by *CMA* and MoM was then calculated:

$$K \approx Average\ [WM\text{-}S/\Delta W] \tag{8}$$

iii. Finally, a general form of the proposed formula, *WM-F* could be calculated as:

$$WM\text{-}F = \left[KWCA/\overline{K}\right] - V \tag{9}$$

iv. where $V = \varepsilon r/2$ represents the value of substrate permittivity divided by 2, whereas $\overline{K}$ represents the value of k with an estimated correction factor (R) which varied between (0.8 to 0.9) for all substrates, calculated as:

$$\overline{K} = K + R \tag{10}$$

v. The deviation between the patch width value in simulation and the proposed formula, D, was used to determine the accuracy of the proposed method, as follows:

$$D = WM\text{-}S - WM\text{-}F \tag{11}$$

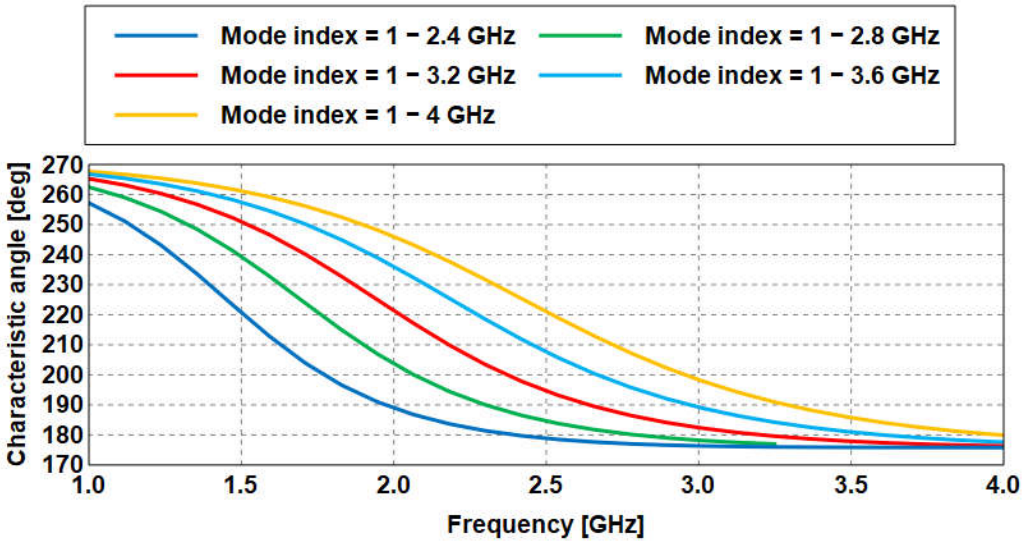

Figure 3. Characteristic angle of a square patch at different operating frequencies.

Next, all calculation results for each substrate were used to estimate a set of customized formulae in Table 2. These simple closed-form formulae provided satisfactory accuracy in estimating the patch dimensions. The rate of deviations in dimensions between the values obtained from the formula and the actual value varied, depending on the operating frequencies, as seen in Figure 4. However, their variations were less than 0.5 mm, which indicated accuracy in estimating the patch dimensions. The proposed formula for each substrate would help a designer estimate the patch's dimension without the effect of substrate, ground, and excitation, saving time needed for analysis.

Table 2. Proposed Formulae for Different Substrate Materials.

Substrate	Proposed Formula
Felt	$WM\text{-}F = (0.7\ WCA) - 0.6$
RO4003C	$WM\text{-}F = (0.52\ WCA) - 1.7$
Denim	$WM\text{-}F = (0.65\ WCA) - 0.85$
Rogers RT/Duroid 5880	$WM\text{-}F = (0.61\ WCA) - 1.1$

A systematic procedure of transforming the patch width obtained using CMA (*WCA*) to the actual value of the width of the antenna (*WM-S*) is summarized in Figure 5. The patch dimensions from each substrate type are presented in Tables 3–6.

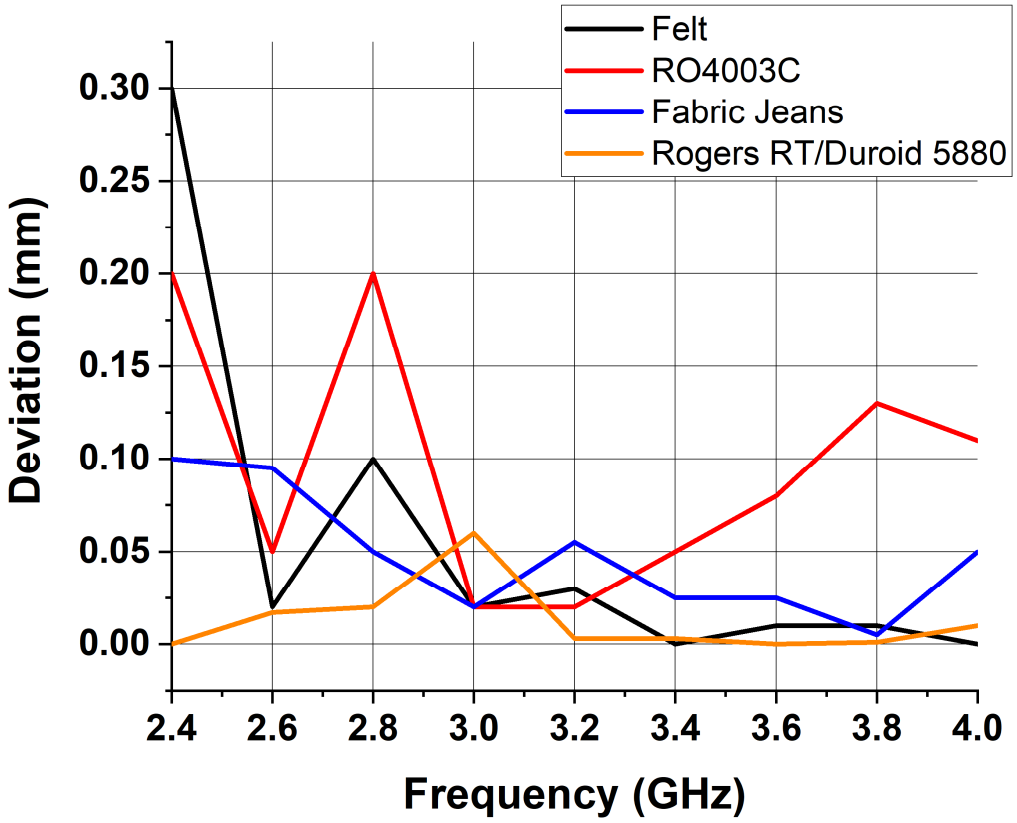

Figure 4. Deviation of results for different substrates.

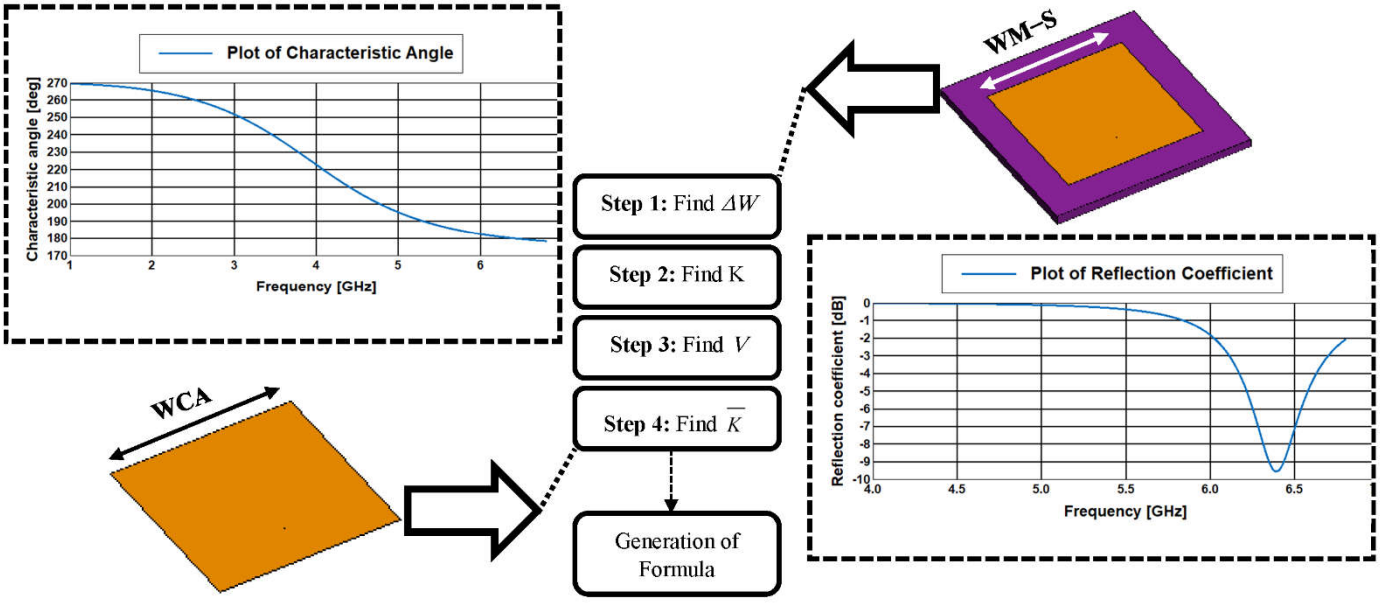

Figure 5. Summary of the formulation process.

Table 3. Patch width estimation on felt substrate using CMA.

f (GHz)	WCA (mm)	WM-S (mm)	ΔW = WCA − WM-S (mm)	K = WM-S/ΔW	WM-F (mm)	D = |WM-S − WM-F| (mm)	Δ Error (%)
2.4	70	48.7	21.3	2.28	48.4	0.3	0.61
2.6	64.7	44.71	19.99	2.23	44.69	0.02	0.04
2.8	60	41.5	18.5	2.24	41.4	0.1	0.24
3.0	56	38.62	17.38	2.22	38.6	0.02	0.05
3.2	52.3	36.04	16.26	2.21	36.01	0.03	0.08
3.4	49.3	33.91	15.39	2.2	33.91	0	0
3.6	46.5	31.96	14.54	2.19	31.95	0.01	0.03
3.8	44.1	30.26	13.84	2.18	30.27	0.01	0.03
4.0	42	28.8	13.2	2.18	28.8	0	0
4.2	39.9	27.2	12.7	2.14	27.33	0.13	0.47
4.4	38.1	26	12.1	2.14	26.07	0.07	0.26
4.6	36.4	24.6	11.8	2.08	24.88	0.28	1.13
4.8	34.7	23.4	11.3	2.07	23.69	0.29	1.23
5.0	33.4	22.6	10.8	2.09	22.78	0.18	0.79
5.2	32.1	21.92	10.2	2.14	21.87	0.03	0.22
5.4	30.9	21	9.9	2.12	21.03	0.03	0.14
5.6	29.8	20.2	9.6	2.1	20.26	0.06	0.29
5.8	28.8	19.5	9.3	2.09	19.56	0.06	0.31
6.0	27.8	18.86	8.94	2.1	18.86	0	0
6.2	26.8	18.2	8.6	2.11	18.16	0.04	0.22
6.4	26	17.7	8.3	2.13	17.6	0.1	0.56
6.6	25.2	17.06	8.14	2.09	17.04	0.02	0.11
12.4	13.45	8.815	4.653	1.9	8.815	0	0

Table 4. Patch width estimation on RO4003C substrate using CMA.

f (GHz)	WCA (mm)	WM-S (mm)	ΔW = WCA − WM-S (mm)	K = WM-S/ΔW	WM-F (mm)	D = |WM-S − WM-F| (mm)	Δ Error (%)
2.4	70	34.5	35.5	0.97	34.7	0.2	0.57
2.6	64.7	31.89	32.81	0.97	31.94	0.05	0.15
2.8	60	29.3	30.7	0.95	29.5	0.2	0.68
3.0	56	27.4	28.6	0.95	27.42	0.02	0.07
3.2	52.3	25.47	26.83	0.94	25.49	0.02	0.07
3.4	49.3	23.88	25.42	0.93	23.93	0.05	0.21
3.6	46.5	22.4	24.1	0.92	22.48	0.08	0.35
3.8	44.1	21.1	23	0.91	21.23	0.13	0.61
4.0	42	20.03	21.97	0.91	20.14	0.11	0.54
4.2	39.9	19	20.9	0.9	19.04	0.04	0.21
4.4	38.1	18	20.1	0.89	18.11	0.11	0.61
4.6	36.4	17.22	19.18	0.89	17.22	0	0
4.8	34.7	16.33	18.37	0.88	16.34	0.01	0.06
5.0	33.4	15.67	17.73	0.88	15.66	0.01	0.06
5.2	32.1	15	17.1	0.87	14.99	0.01	0.06
5.4	30.9	14.21	16.69	0.85	14.36	0.15	1.05
5.6	29.8	13.66	16.14	0.84	13.79	0.13	0.94
5.8	28.8	13.3	15.5	0.85	13.27	0.03	0.22
6.0	27.8	12.63	15.17	0.83	12.79	0.12	1.25
6.2	26.8	12.24	14.56	0.84	12.23	0.01	0.08
6.4	26	11.83	14.17	0.83	11.82	0.01	0.08
6.6	25.2	11.41	13.79	0.82	11.4	0.01	0.08
12.4	13.45	5.8	7.65	0.75	5.29	0.51	9.19

Table 5. Patch width estimation on denim substrate using CMA.

f (GHz)	WCA (mm)	WM-S (mm)	ΔW = WCA − WM-S (mm)	K = WM-S/ΔW	WM-F (mm)	D = |WM-S − WM-F| (mm)	Δ Error (%)
2.4	70	44.75	25.25	1.77	44.65	0.1	0.22
2.6	64.7	41.3	23.4	1.76	41.205	0.095	0.23
2.8	60	38.2	21.8	1.75	38.15	0.05	0.13
3.0	56	35.57	20.43	1.74	35.55	0.02	0.05
3.2	52.3	33.2	19.1	1.73	33.143	0.055	0.17
3.4	49.3	31.22	18.08	1.72	31.195	0.025	0.08
3.6	46.5	29.4	17.1	1.71	29.375	0.025	0.08
3.8	44.1	27.82	16.28	1.7	27.815	0.005	0.01
4.0	42	26.5	15.5	1.7	26.45	0.05	0.18
4.2	39.9	25.1	14.8	1.69	25.085	0.015	0.05
4.4	38.1	23.92	14.18	1.68	23.915	0.005	0.02
4.6	36.4	22.84	13.56	1.68	22.81	0.03	0.13
4.8	34.7	21.58	12.82	1.68	21.51	0.07	0.32
5.0	33.4	20.88	12.52	1.66	20.86	0.02	0.09
5.2	32.1	20.02	12.08	1.65	20.015	0.005	0.02
5.4	30.9	19.3	11.6	1.66	19.235	0.065	0.33
5.6	29.8	18.6	11.2	1.66	18.521	0.08	0.42
5.8	28.8	18	10.8	1.66	17.87	0.13	0.72
6.0	27.8	17.23	10.57	1.63	17.22	0.01	0.05
6.2	26.8	16.58	10.22	1.62	16.57	0.01	0.06
6.4	26	16.06	9.94	1.61	16.05	0.01	0.06
6.6	25.2	15.54	9.66	1.6	15.53	0.01	0.06
12.4	13.45	7.88	5.57	1.41	7.89	0.01	0.12

Table 6. Patch width estimation on Rogers RT/Duroid 5880 substrate using CMA.

f (GHz)	WCA (mm)	WM-S (mm)	ΔW = WCA − WM-S (mm)	K = WM-S/ΔW	WM-F (mm)	D = |WM-S − WM-F| (mm)	Δ Error (%)
2.4	70	41.6	28.4	1.46	41.6	0	0
2.6	64.7	38.35	26.35	1.45	38.367	0.017	0.04
2.8	60	35.48	24.52	1.44	35.5	0.02	0.05
3.0	56	33	23	1.43	33.06	0.06	0.18
3.2	52.3	30.8	21.5	1.43	30.803	0.003	0.01
3.4	49.3	28.97	20.33	1.42	28.973	0.003	0.01
3.6	46.5	27.265	19.235	1.41	27.265	0	0
3.8	44.1	25.8	18.3	1.4	25.801	0.001	0.003
4.0	42	24.51	17.49	1.4	24.52	0.01	0.04
4.2	39.9	23	16.4	1.4	22.934	0.066	0.28
4.4	38.1	22.141	15.959	1.38	22.141	0	0
4.6	36.4	21.104	15.296	1.37	21.104	0	0
4.8	34.7	20.1	14.3	1.4	19.884	0.216	1.08
5.0	33.4	19.2	14.2	1.35	19.274	0.074	0.38
5.2	32.1	18.21	13.89	1.31	18.481	0.271	1.47
5.4	30.9	17.7	13.2	1.34	17.749	0.049	0.27
5.6	29.8	17.27	12.53	1.37	17.078	0.192	1.11
5.8	28.8	16.63	12.17	1.36	16.468	0.162	0.97
6.0	27.8	15.86	11.94	1.32	15.858	0.002	0.01
6.2	26.8	15.25	11.55	1.32	15.248	0.002	0.01
6.4	26	14.77	11.23	1.31	14.76	0.01	0.06
6.6	25.2	14.22	10.92	1.3	14.272	0.052	0.36
12.4	13.45	7.506	5.944	1.26	7.105	0.401	5.48

2.2. Slotted Antenna

To extend the proposed method to include dimensions of patches with multiple slots, two cases of slotted antennas were further validated. A square patch was integrated with either: (i) a centered rectangular slot (CRS), or (ii) a pair of parallel rectangular slots (PRSs). Their dominant modes were excited to estimate their operating frequencies when designed on different substrates.

2.2.1. Center Rectangular Slot (CRS)

In this section, a simple rectangular slot dimensioned at Lc = 4 mm × Wc = 25 mm was centered on a square patch with a distance of $S1$ = 31.94 mm and $S2$ = 20.99 mm from its edges, as shown in Figure 6.

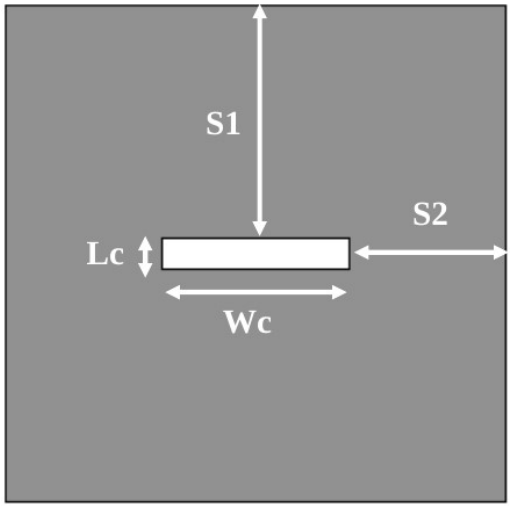

Figure 6. Patch with CRS structure.

Formulae for this structure, using different substrate materials, were generated, and are presented in Table 2. The transformation process of the slotted patch width-based CMA to the actual value used in the complete antenna was first performed for the felt substrate. It was observed that a similar value of the resonant frequency (fr) of 2.26 GHz was produced by full-wave analysis, hence validating the formula (see Figure 7a). Next, in Figure 7b, a slight difference (of 10 MHz, 0.46%) was seen between the resonant frequencies resulting from the use of this formula (2.17 GHz) compared to the full-wave analysis (2.18 GHz) for a denim substrate. A larger difference (60 MHz, 38.96%) was observed for the last two substrates (RO4003C and Rogers 5880), as illustrated in Figure 7c,d. These differences were potentially caused by the mesh size, feed location, and dimensions of the substrate/ground. Furthermore, the resonance of slotted antennas could also be dependent on mode 2, rather than mode 1. While the first two modes are the dominant modes excited in most structures, the resonance variation of different dominant modes might cause slight differences in the estimated physical patch dimensions.

2.2.2. Parallel Rectangular Slots (PRSs)

Another set of investigations was performed on another antenna topology to validate the proposed formulae. The same patch structure from the previous was integrated with a pair of parallel rectangular slots. Each slot was dimensioned at Lr = 30 mm × Wr = 4 mm, with a spacing of d = 20 mm between them. They were located from the patch at a distance of $S3$ = 18 mm and $S4$ = 19.49 mm, as depicted in Figure 8.

FEKO simulations of this antenna on a felt substrate produced a resonant frequency of 2.25 GHz; and this value was higher than the theoretical value of 2.06 GHz produced by the formula (see Figure 9a). Next, using denim and RO4003C substrates, the difference between the resonant frequencies from each respective step produced 230 MHz and 160 MHz, 11.14%

and 9.20%, respectively, as shown in Figure 9b,c. Finally, for the Rogers 5880 substrate, the difference between the proposed approach and the full-wave analysis was 200 MHz, 10.1%, as illustrated in Figure 9d. All calculated *fr* results from the two methods and two patches (with CRS and PRS) using the four different substrates are summarized in Table 7. The reason for the difference was due to several factors, as follow. Firstly, the resulting resonant frequencies obtained were highly dependent on the surface wave. These waves propagating through a finite antenna can be used to add another resonance to the antenna system, thus, significantly improving antenna bandwidth. Besides that, the ground/substrate dimensions relative to the patch caused variations in resonant frequency. Typically, the length/width of the patch is about six times the height of the substrate. Finally, the mesh size chosen in simulations significantly impacts the results. Therefore, this work adopted the highest resolution of mesh sizes to analyze the antenna structure and generate the data used to define the formula.

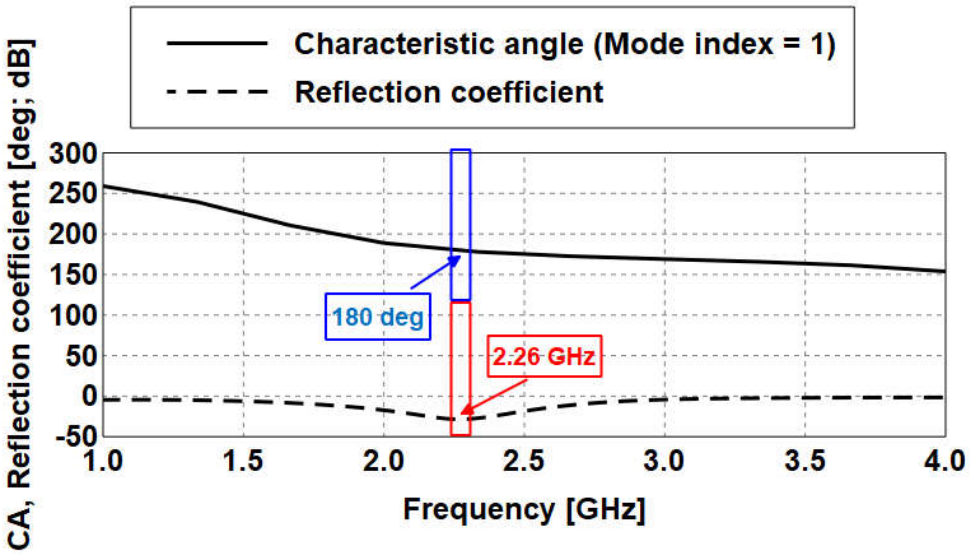

(**a**)

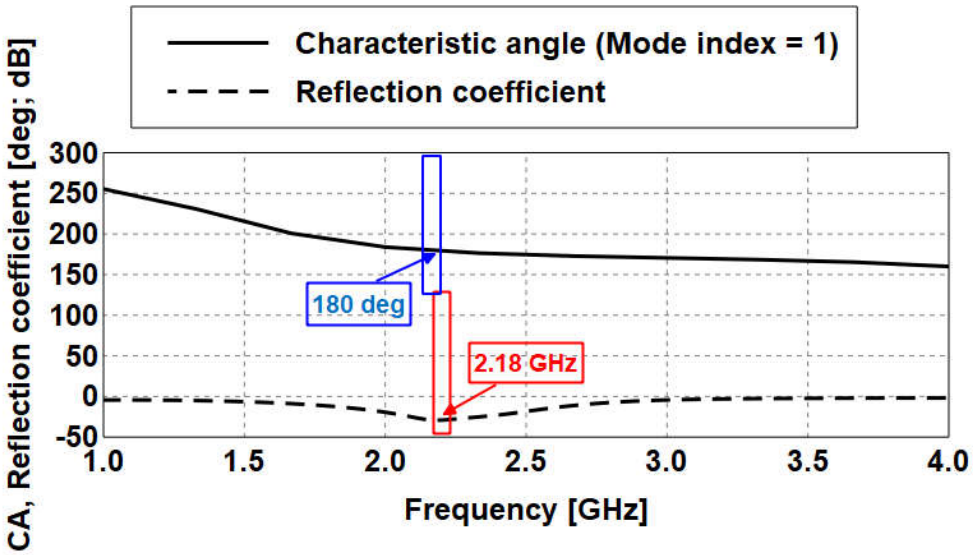

(**b**)

Figure 7. *Cont.*

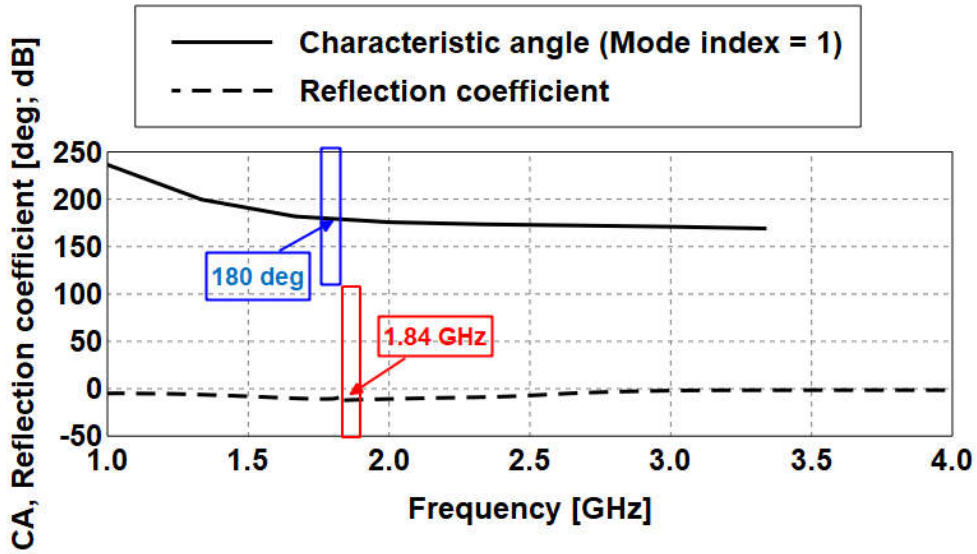

(**c**)

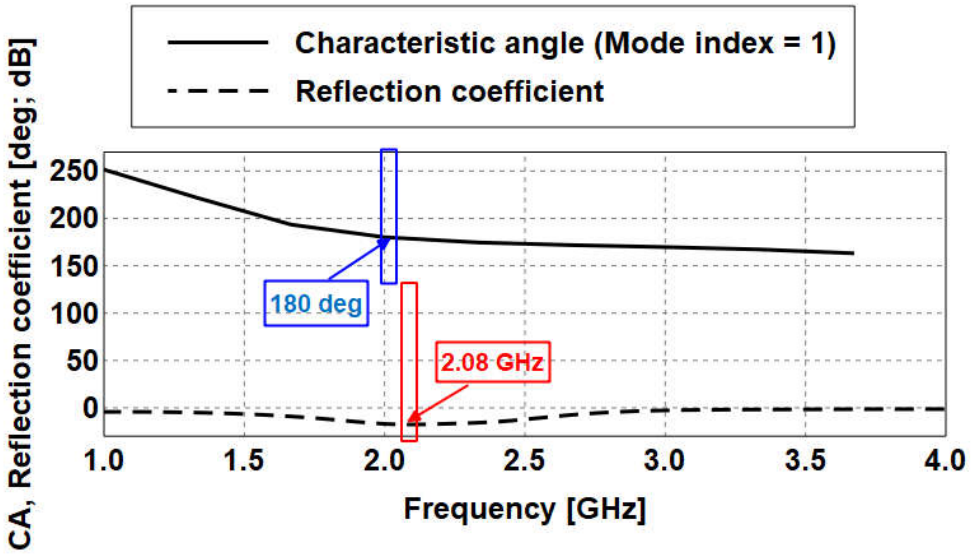

(**d**)

Figure 7. Characteristic angle and reflection coefficients of the patch with CRS on different substrates: (**a**) felt (**b**) denim (**c**) RO4003C (**d**) Rogers 5880.

Table 7. Overall Results of CRS and PRSs Antennas.

Substrate Material		WCA (mm)	fr (Formula) (GHz)	fr (Full Wave Analysis) (GHz)	Difference (MHz)/(%)
Felt	CRS	66.98	2.26	2.26	0
	PRSs		2.06	2.25	190/9.22
Denim	CRS	72.52	2.17	2.18	10/0.46
	PRSs		1.95	2.18	230/10.55
RO4003C	CRS	92.28	1.78	1.84	60/3.37
	PRSs		1.66	1.82	160/9.63
Rogers 5880	CRS	77.68	2.02	2.08	60/2.97
	PRSs		1.88	2.08	200/10.63

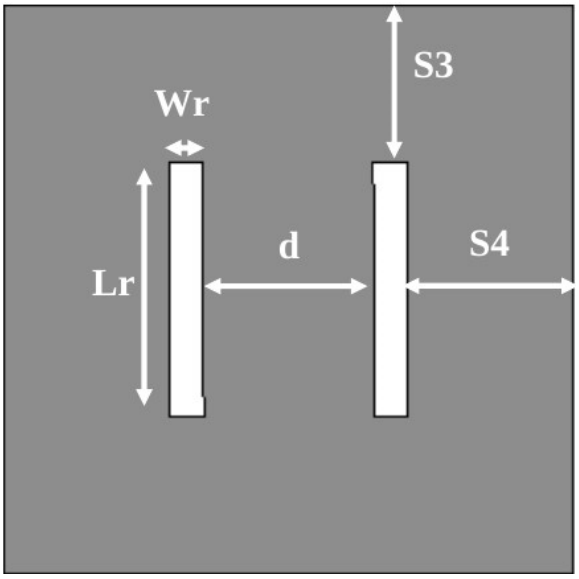

Figure 8. Patch with PRSs structure.

Table 8 compares the proposed approach with other methods available in the literature concerned with designing RMSAs. It can be seen that this method provided a quick estimation for the width of the radiator patch using only CMA, without considering the effects of substrate and excitation.

Table 8. Comparison of the proposed method with other approaches in literature.

Ref	Study	Method Used	Required Parameters for Calculation	Parameters Estimated
[20]	Calculation of a rectangular patch dimension.	Transmission line model.	- Dielectric constant. - Substrate thickness. - Operating frequency	Patch length and width.
[21–23]	Calculation of a rectangular patch dimension.	Equivalency of designs.	- Normalized substrate thickness. - Electric length of the patch (dictated by the required fr).	Patch length.
[24]	Calculation of a rectangular patch dimension.	Curve fittingtechnique (CFT).	- Substrate thickness. - Dielectric constant. - Resonant frequency	Patch length and width.
[25]	Calculating the resonant frequency of patch antenna.	Taguchi method.	- Velocity of electromagnetic waves in free space. - Effective dielectric constant. - Effective length and width. - Integer values (m and n)	Resonant frequency of rectangular antenna.
[26,27]	Calculation of a rectangular patch dimension.	Iterative process.	- Dielectric constant. - Thickness of the substrate. - Patch length and width. - Feed-point location.	Patch length and width.
[28]	Calculation of a slot dimension in the rectangular antenna	Transmission line model.	- Width of the patch. - Substrate thickness. - Dielectric constant.	Length and width of the slot in the antenna
This paper	Calculation of a square/ rectangular patch dimension.	Characteristic mode analysis.	Width of the patch based on CMA.	Patch width/length

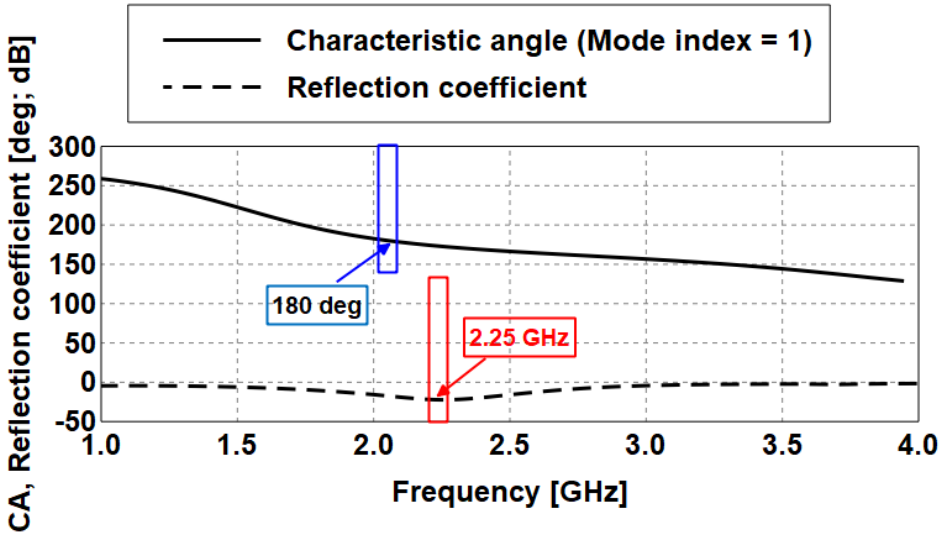

(**a**)

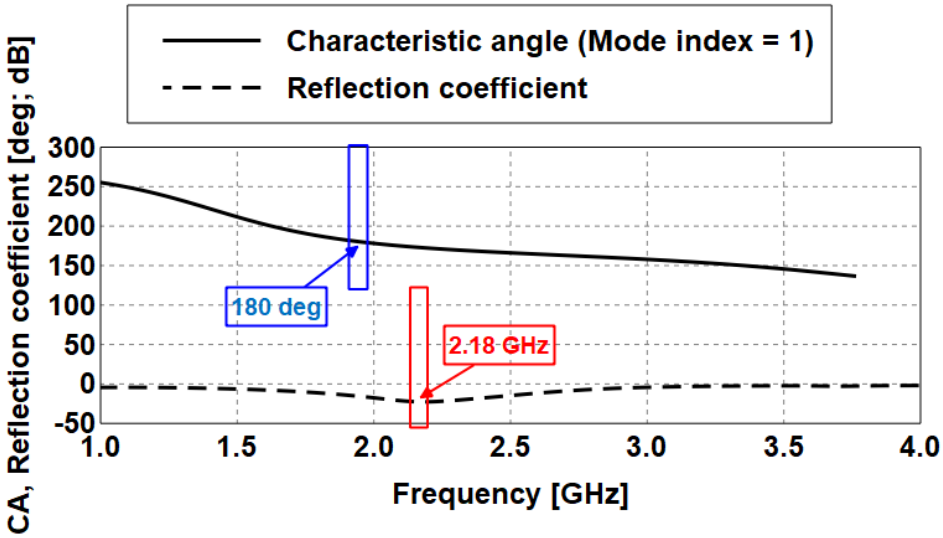

(**b**)

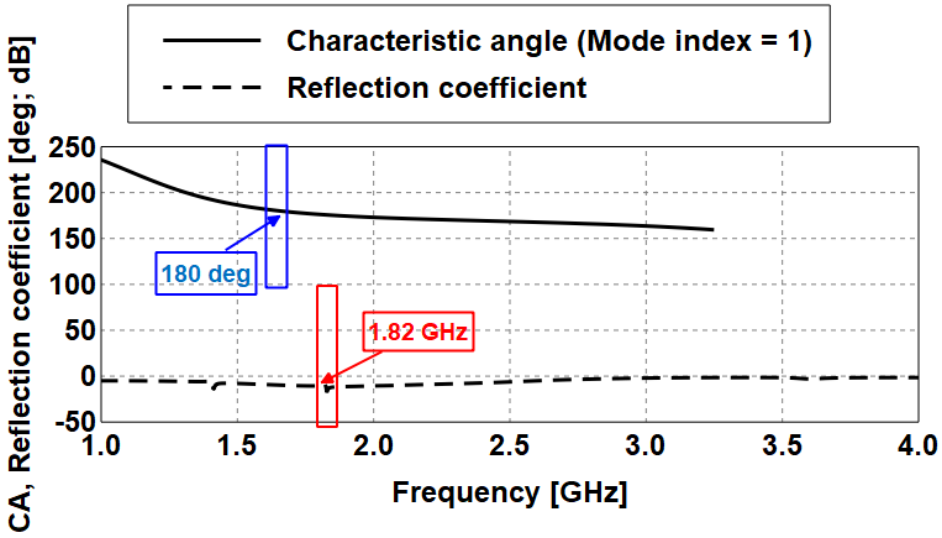

(**c**)

Figure 9. *Cont.*

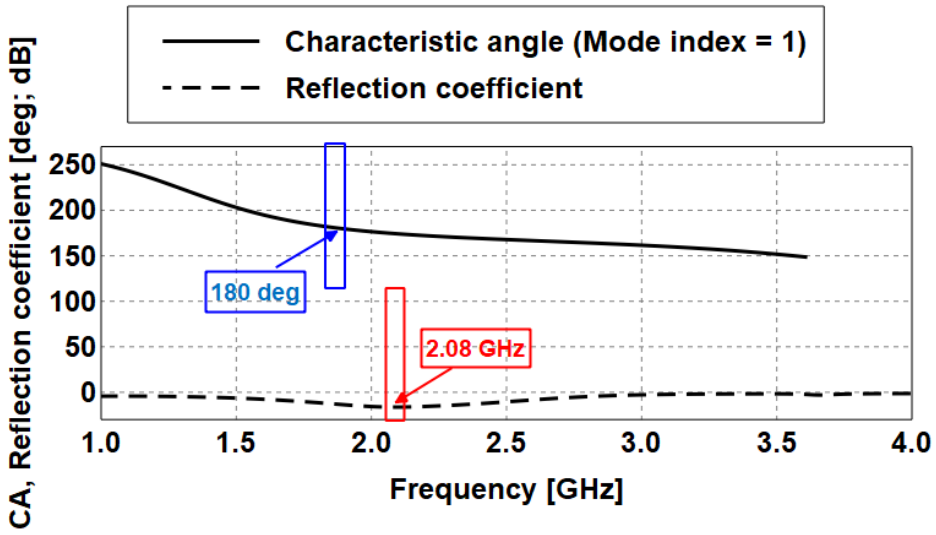

(**d**)

Figure 9. Characteristic angle and reflection coefficient of the patch with PRSs on different substrates: (**a**) Felt (**b**) Denim (**c**) RO4003C (**d**) Rogers 5880.

3. Application to a Dual Band Slot Antenna

In this section, a new coplanar waveguide (CPW)-fed dual-band antenna was designed using the proposed method. First, the dimensions of the rectangular patch were estimated using the proposed empirical formula. The dimensions of the rectangular patch were transformed from LCA = 58 mm × WCA = 44 mm (0.47 λo × 0.35 λo) to $LM\text{-}S$ = 40 mm × $WM\text{-}S$ = 30.2 mm (0.32 λo × 0.24 λo), using the formula derived and using the felt substrate at 2.45 GHz, as shown in Figure 10. The proposed antenna was then designed on top of a textile substrate which had a εr of 1.3, thickness (h) of 3 mm, and a tanδ of 0.044 (see Figure 11). The patch was made of a ShieldIt SuperTM conductive textile, with its dimensions summarized in Table 9.

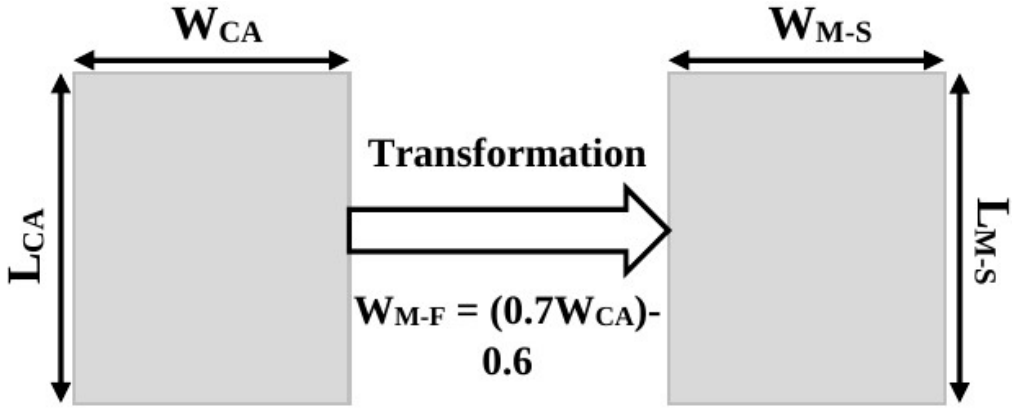

Figure 10. Transformation process of the patch dimensions.

Table 9. Dual Band Antenna Dimensions.

Parameter	Value (mm)	Parameter	Value (mm)
W1	90	*L1*	100
W2	78	*L2*	30
W3	4	*L3*	42
W4	5	*L4*	6
W5	39.5	*L5*	8

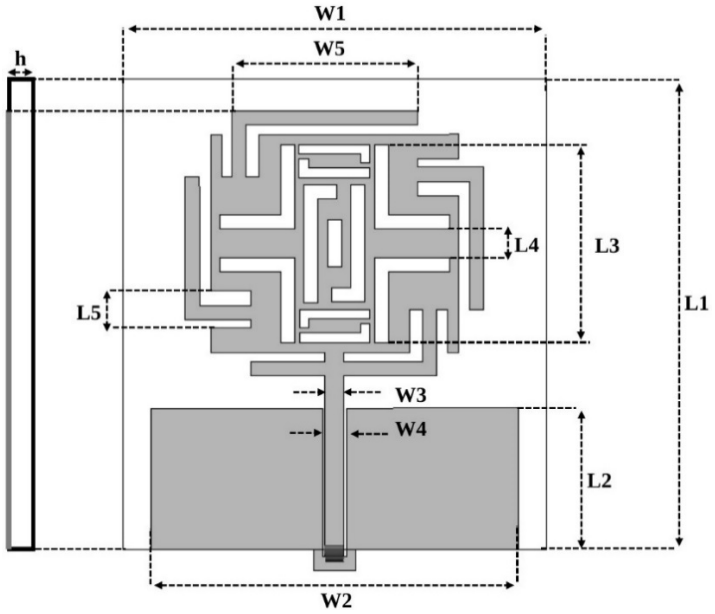

Figure 11. Layout of the dual band wearable antenna.

The proposed antenna was designed in four steps (see Figure 12) to achieve the target operation at 2.45 GHz more accurately and to improve the antenna performance.

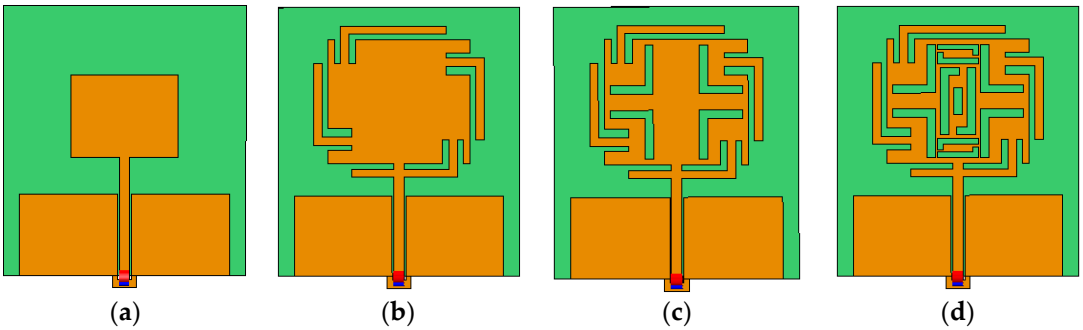

Figure 12. Dual band antenna design stages: (**a**) Step 1 (**b**) Step 2 (**c**): Step 3 (**d**) Step 4.

The conventional RMSA (denoted as Step 1 in Figure 12a) resulted in an impedance bandwidth of 228 MHz with a minimum reflection coefficient of −10.55 dB at 2.25 GHz. Next, several rectangular slots were integrated near the patch edges, which further extended the size of the antenna, as shown in Figure 12b. The proposed method was shown to be effective in estimating the dimensions of the antenna for operation at 2.45 GHz. This was seen by the close-to-180° value of its CA at 2.45 GHz, as specified in the proposed design procedure. The patch dimensions were 91.47 mm × 81.31 mm (0.75 λo × 0.66 λo), as seen in Figure 13. These dimensions were then transformed to new values using the proposed method to factor in the presence of the substrate and excitation, as depicted in Figure 14. The resulting overall antenna size with slots upon this transformation process was 63.43 mm × 56.32 mm (0.52 λo × 0.46 λo). Its bandwidth was enhanced to more than 760 MHz at 2.45 GHz, with an additional resonance at 3.44 GHz. Reflection coefficients of the antenna from the first two steps are illustrated in Figure 15.

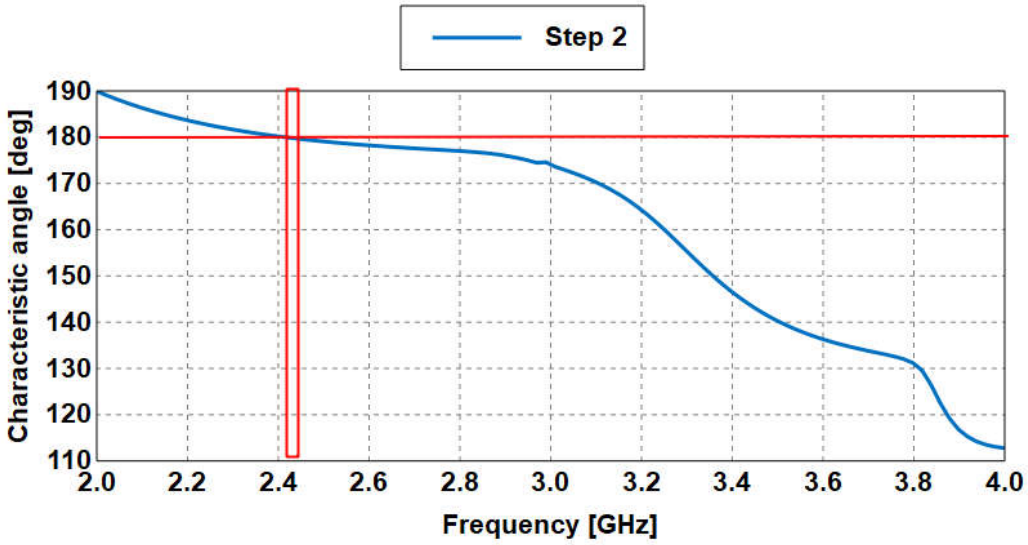

Figure 13. CA of Step 2 of the proposed design (mode 1).

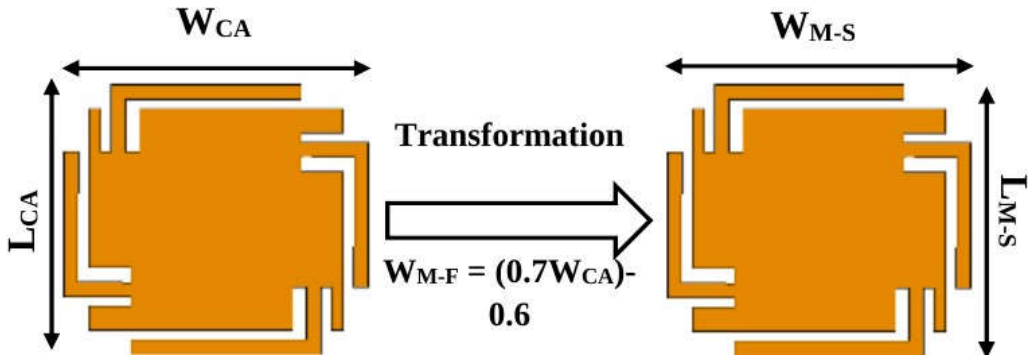

Figure 14. Transformation process of the patch dimensions at Step 2 of the design process.

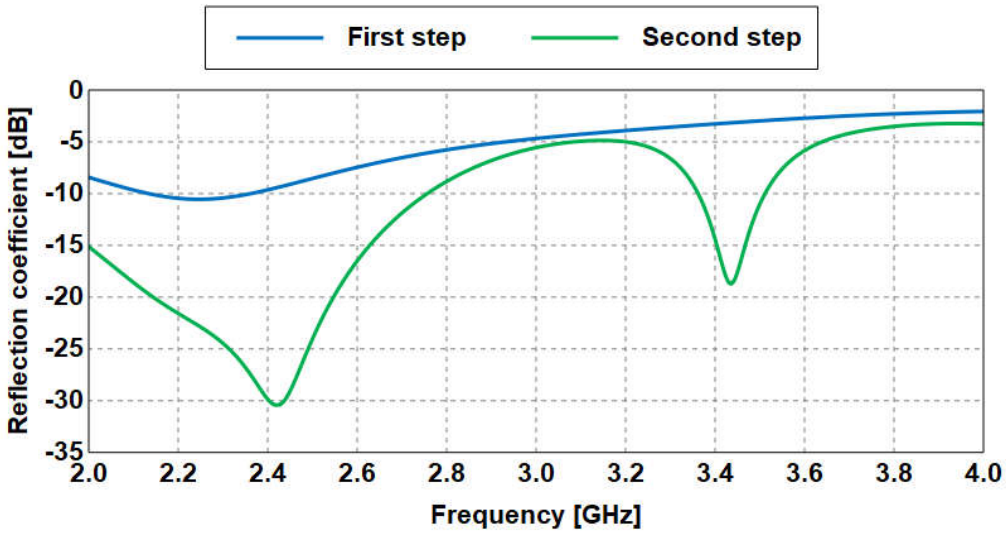

Figure 15. Reflection coefficients of Steps 1 and 2 of the proposed method in designing the dual band slot antenna.

The increasing complexity of the slot in the patch may excite other dominant modes, instead of the fundamental modes, due to the changing current distribution along the surface of the radiator caused by the additional slots. This can be seen in Figure 16, where

the CA for mode 5 was close to 180° after steps 3 and 4 of the design process. Hence, the patch dimensions could also be transformed at these steps using the proposed formula, based on the CA results of this mode (see Figure 17a,b). The deviation values at steps 3 and 4 were115 MHz and 20 MHz, 4.81% and 0.82%, respectively.

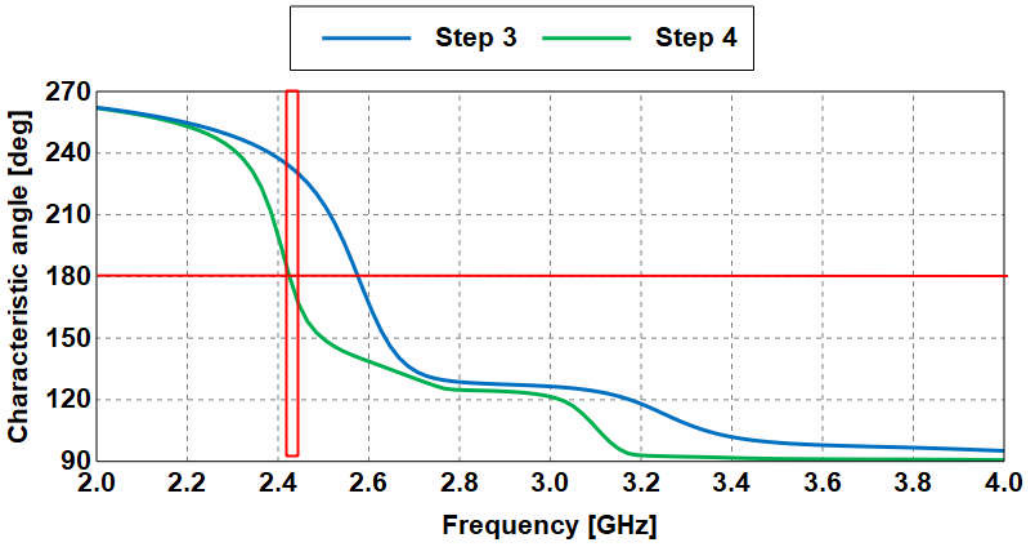

Figure 16. CA results of Steps 3 and 4 of the proposed design—mode 5.

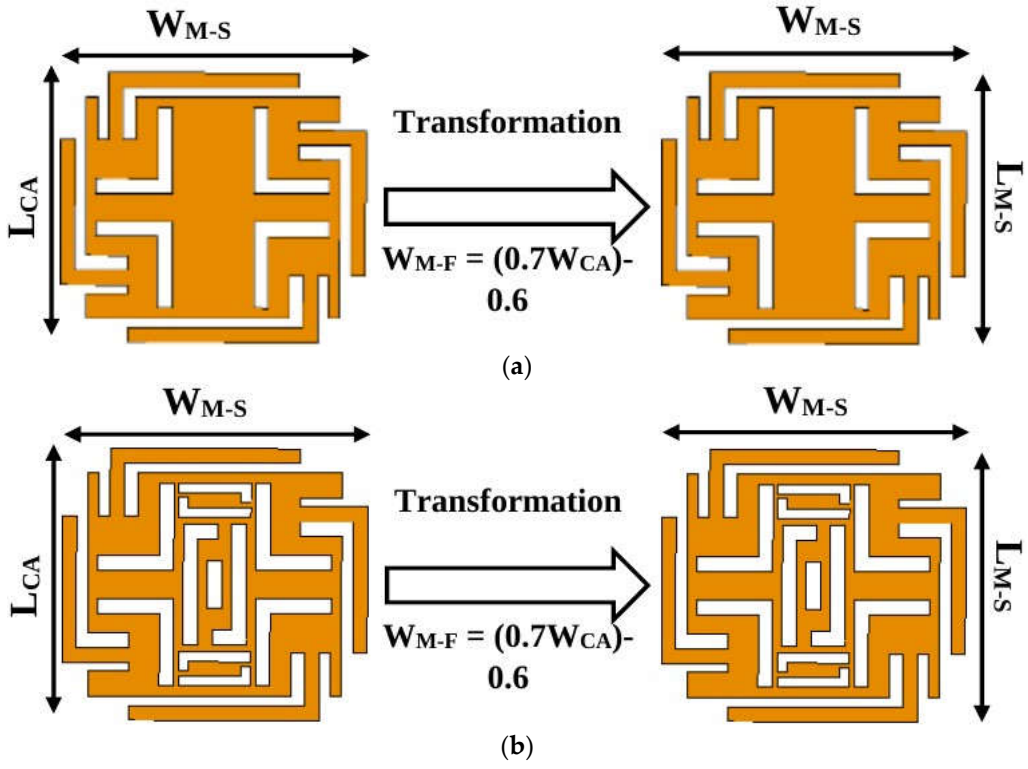

Figure 17. Transformation process of the patch dimensions (**a**) step 3 (**b**) step 4.

The satisfactory convergence of the reflection coefficient for steps 3 and 4 can be observed in Figure 18, whereas Figure 19 shows the 3D realized gain of 3 dBi and 6 dBi, respectively, for each step. The differences in realized gain were attributed to the modified surface current, due to the additional slots on the patch.

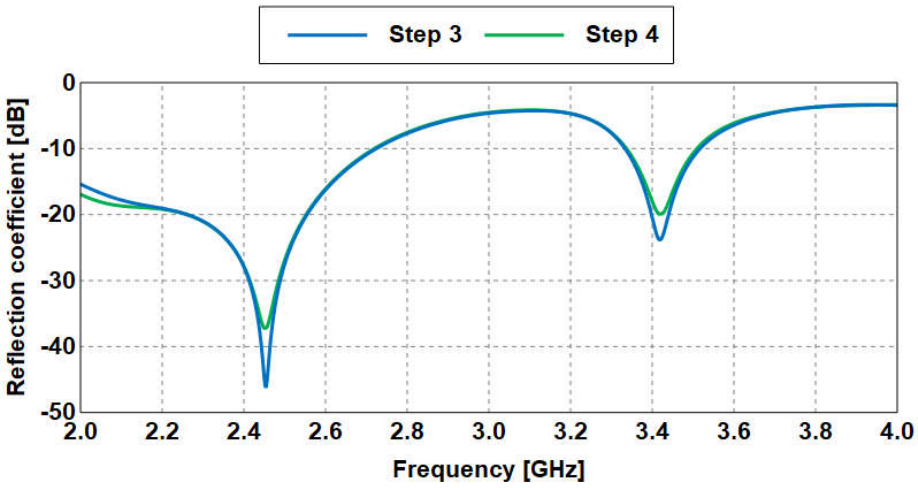

Figure 18. Reflection coefficients of Steps 3 and 4 of the proposed method in designing the dual band slot antenna.

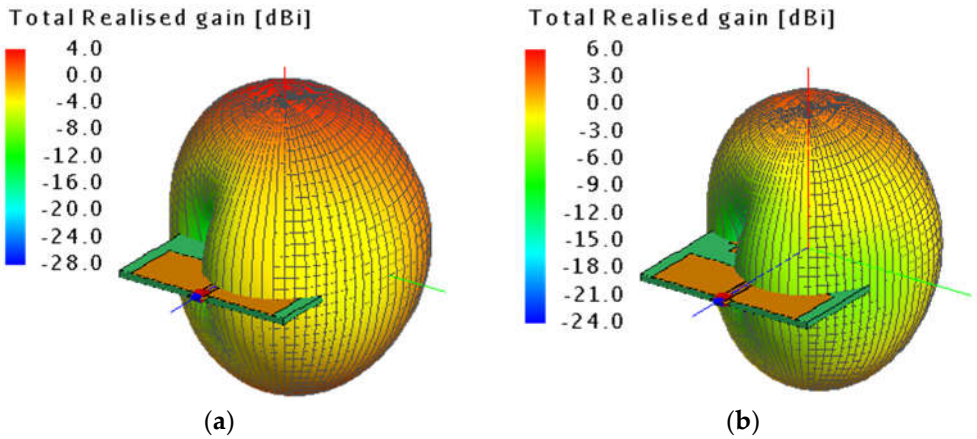

(**a**) (**b**)

Figure 19. Realized gain at 2.45 GHz for (**a**) step 3 (**b**) step 4.

Upon the connection of the feed line to the patch, the structure was analyzed in terms of modal significance (MS), a normalized amplitude of the current modes. Using this parameter, a mode was resonant when its modal significance was at least 0.7. The closer the modal significance was to unity, the more efficiently the mode resonated and radiated when excited. The resonant frequencies of the modes for each step of the antenna design are shown in Figure 20 and are summarized in Table 10.

Table 10. Resonant Frequencies of modes for Each Design Step of The Dual Band Antenna Design Using CMA.

Step	Resonant Frequency (GHz)
Step 1	2.63 3.81
Step 2	2.9
Step 3	2.48 3.48
Step 4	2.33 3.42

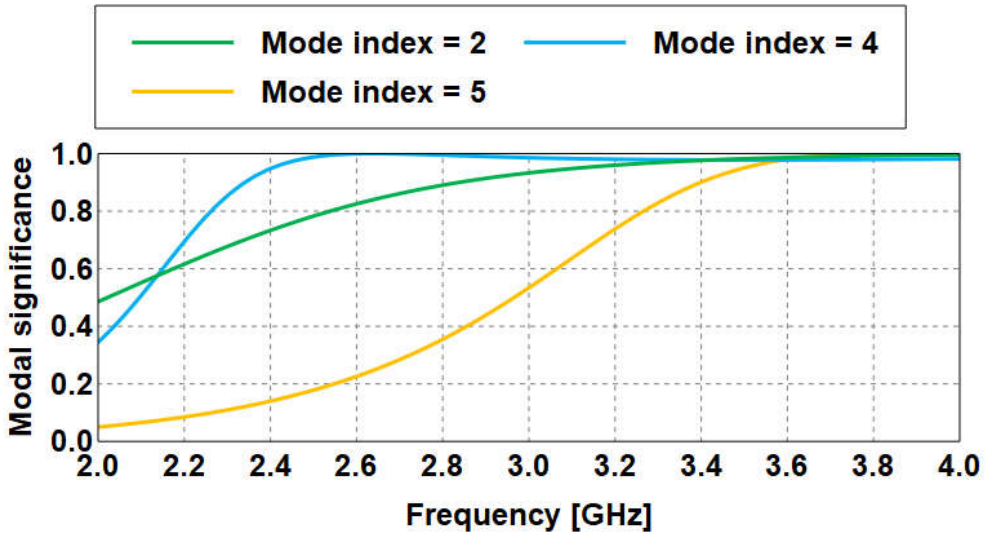

(**a**)

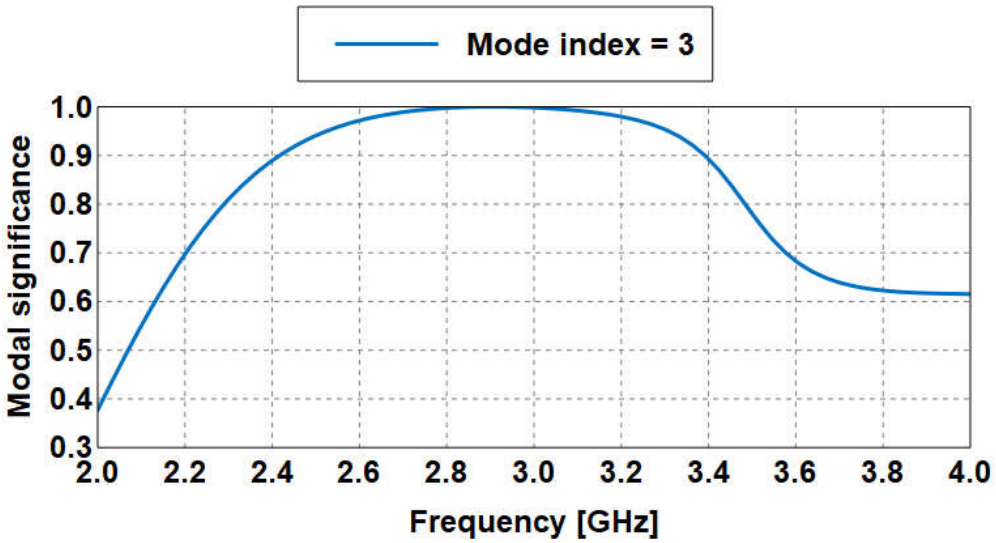

(**b**)

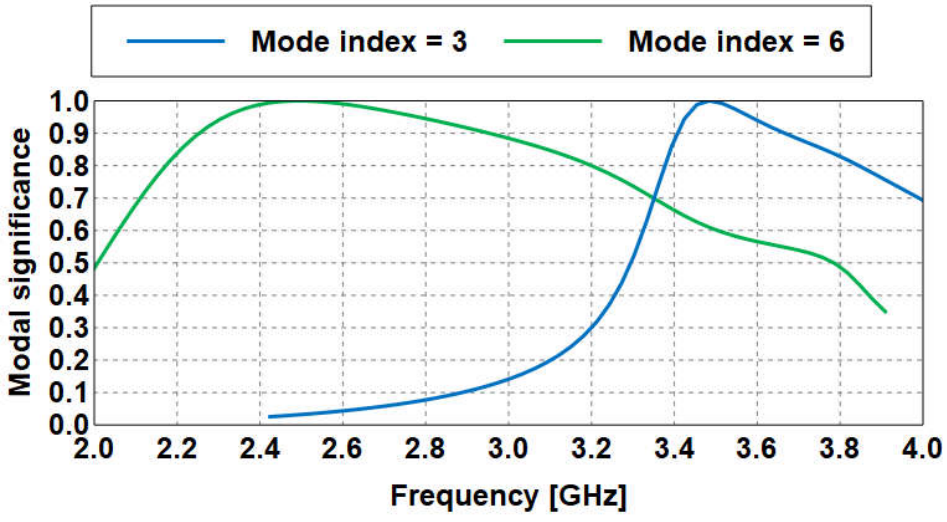

(**c**)

Figure 20. *Cont*.

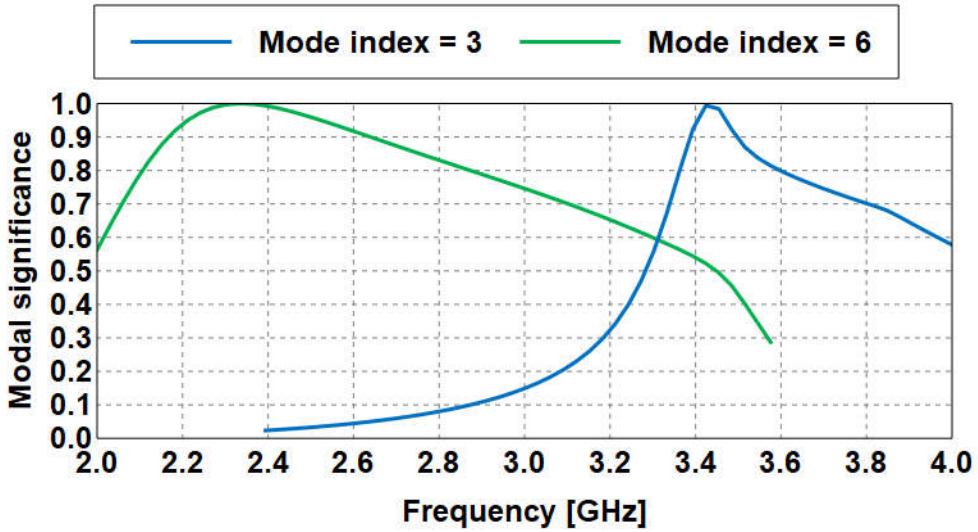

(**d**)

Figure 20. Modal significance for each step of the dual band antenna design (**a**) step 1 (**b**) step 2 (**c**) step 3 and (**d**) step 4.

To validate this method, the proposed antenna was then fabricated, as shown in Figure 21a. A manual cutting technique was used to dimension each antenna layer prior to evaluation using a vector network analyzer (Anritsu model S362E), as depicted in Figure 21b. Figure 22 shows the simulated and measured reflection coefficients for this antenna prototype, which were in good agreement and had a reflection coefficient of less than −10 dB. Differences between the measurement results and simulations were due to factors such as the difference in material properties in practice, and inevitable movements due to the flexibility of the structure. However, the desired operating ranges were achieved.

(**a**) (**b**)

Figure 21. (**a**) Fabricated dual band antenna, (**b**) measured reflection coefficients.

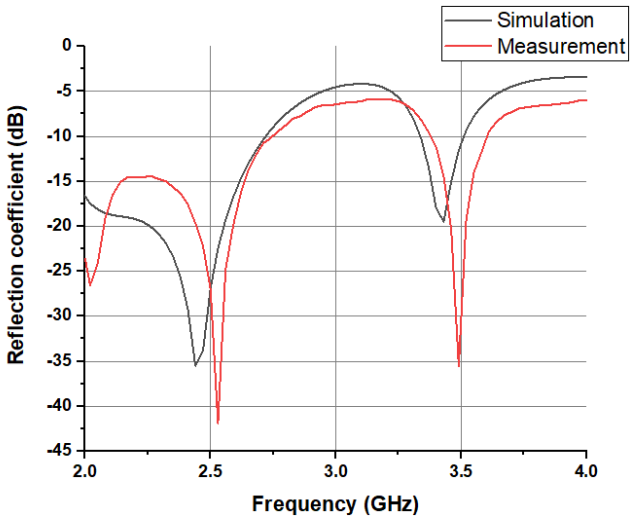

Figure 22. Simulated and measured reflection coefficients of the dual band textile antenna designed using this method.

4. Conclusions

In this paper, a new procedure, based on the CMA technique, for quick estimation of patch antenna dimensions on different substrates was presented. For every antenna type, four steps were proposed to first introduce a curve-fitting formula to find the relationship between the variables obtained at different resonant frequencies. This then enables the quick estimation of the dimensions of the patch, using CMA, without including the substrate and excitation. Only four steps are needed to apply these formulae in estimating the dimensions of other more sophisticated designs. This supports the validity and simplicity of the formula presented in this study for electrically thin and thick MSAs, compared with other approaches in the literature. Furthermore, the proposed expression is suitable to design slotted antennas, with an average difference of 10%. As a final validation, a flexible CPW-fed antenna was designed based on this method. The dual-band antenna designed using this approach operated at 2.33 and 3.42 GHz with a minimum reflection coefficient of −35.1 and −19.2 dB, respectively. Its gains were improved by 6 and 3 dBi at 2.33 and 3.42 GHz, respectively, with simulations and measurement results showing satisfactory agreements.

Author Contributions: Conceptualization, B.B.Q.E. and P.J.S.; methodology, B.B.Q.E.; validation, B.B.Q.E. and P.J.S.; resources, A.A.A.-H. and P.A.; writing—original draft preparation, B.B.Q.E.; writing—review and editing, P.J.S., A.A.A.-H. and P.A.; supervision, P.J.S. and A.A.A.-H.; funding acquisition, P.J.S. All authors have read and agreed to the published version of the manuscript.

Funding: This work has been funded in part by the Fundamental Research Grant Scheme (grant no: FRGS/1/2020/TK0/UNIMAP/02/19) from the Malaysian Ministry of Higher Education, in part by the National Science, Research and Innovation Fund (NSRF), the King Mongkut's University of Technology North Bangkok (contract no: KMUTNB-FF-66-10), in part by the Academy of Finland 6G Flagship (grant no: 318927), and in part by the Academy of Finland's LiBERATE project (grant no: 346949).

Data Availability Statement: Data supporting reported results may be obtained by contacting the corresponding author.

Conflicts of Interest: The authors declare no conflict of interest.

References

1. Zerith, M.A.T.; Nesasudha, M. A Compact Wearable 2.45 GHz Antenna for WBAN Applications. In Proceedings of the 2020 5th International Conference on Devices, Circuits and Systems (ICDCS), Coimbatore, India, 5–6 March 2020; pp. 184–187. [CrossRef]
2. Sabban, A. Small New Wearable Antennas for IOT, Medical and Sport Applications. In Proceedings of the 2019 13th European Conference on Antennas and Propagation (EuCAP), Krakow, Poland, 31 March–5 April 2019; pp. 1–5.
3. Yang, X.; Fan, D.; Ren, A.; Zhao, N.; Alam, M. 5G-Based User-Centric Sensing at C-Band. *IEEE Trans. Ind. Inform.* **2019**, *15*, 3040–3047. [CrossRef]
4. Yang, X.; Shah, S.A.; Ren, A.; Zhao, N.; Zhang, Z.; Fan, D.; Zhao, J.; Wang, W.; Ur-Rehman, M. Freezing of Gait Detection Considering Leaky Wave Cable. *IEEE Trans. Antennas Propag.* **2019**, *67*, 554–561. [CrossRef]
5. Li, S.; Li, J. Smart Patch Wearable Antenna on Jeans Textile for Body Wireless Communication. In Proceedings of the 2018 12th International Symposium on Antennas, Propagation and EM Theory (ISAPE), Hangzhou, China, 3–6 December 2018; pp. 1–4. [CrossRef]
6. Singh, N.; Singh, V.; Saini, R.; Saini, J.P.; Bhoi, A. Microstrip Textile Antenna with Jeans Substrate with Applications in S-band. In *Advances in Communication, Devices and Networking*; Springer: Singapore, 2018; pp. 369–376. [CrossRef]
7. Garbacz, R.; Turpin, R. A Generalized Expansion for Radiated and Scattered Fields. *IEEE Trans. Antennas Propag.* **1971**, *19*, 348–358. [CrossRef]
8. Harrington, R.; Mautz, J. Theory of Characteristic Modes for Conducting Bodies. *IEEE Trans. Antennas Propag.* **1971**, *19*, 622–628. [CrossRef]
9. Harrington, R.; Mautz, J. Computation of Characteristic Modes for Conducting Bodies. *IEEE Trans. Antennas Propag.* **1971**, *19*, 629–639. [CrossRef]
10. Tran, H.H.; Nguyen-Trong, N.; Abbosh, A.M. Simple Design Procedure of a Broadband Circularly Polarized Slot Monopole Antenna Assisted by Characteristic Mode Analysis. *IEEE Access* **2018**, *6*, 78386–78393. [CrossRef]
11. Vogel, M.; Gampala, G.; Ludick, D.; Jakobus, U.; Reddy, C.J. Characteristic Mode Analysis: Putting Physics back into Simulation. *IEEE Antennas Propag. Mag.* **2015**, *57*, 307–317. [CrossRef]
12. Kim, D.; Nam, S. Systematic Design of a Multiport MIMO Antenna with Bilateral Symmetry Based on Characteristic Mode Analysis. *IEEE Trans. Antennas Propag.* **2018**, *66*, 1076–1085. [CrossRef]
13. Dicandia, F.A.; Genovesi, S. Characteristic Modes Analysis of Non-Uniform Metasurface Superstrate for Nanosatellite Antenna Design. *IEEE Access* **2020**, *8*, 176050–176061. [CrossRef]
14. Li, T.; Chen, Z.N. Wideband Sidelobe-Level Reduced Ka-Band Metasurface Antenna Array Fed by Substrate-Integrated Gap Waveguide Using Characteristic Mode Analysis. *IEEE Trans. Antennas Propag.* **2020**, *68*, 1356–1365. [CrossRef]
15. Shih, T.; Behdad, N. Bandwidth Enhancement of Platform-Mounted HF Antennas Using the Characteristic Mode Theory. *IEEE Trans. Antennas Propag.* **2016**, *64*, 2648–2659. [CrossRef]
16. Dicandia, F.A.; Genovesi, S.; Monorchio, A. Efficient Excitation of Characteristic Modes for Radiation Pattern Control by Using a Novel Balanced Inductive Coupling Element. *IEEE Trans. Antennas Propag.* **2018**, *66*, 1102–1113. [CrossRef]
17. Ren, K.; Nikkhah, M.R.; Behdad, N. Design of Dual-Polarized, Platform-Based HF Antennas Using the Characteristic Mode Theory. *IEEE Trans. Antennas Propag.* **2020**, *68*, 5130–5141. [CrossRef]
18. Ignatenko, M.; Filipovic, D.S. Application of Characteristic Mode Analysis to HF Low Profile Vehicular Antennas. In Proceedings of the IEEE Antennas and Propagation Society International Symposium (APSURSI), Memphis, TN, USA, 6–11 July 2014. [CrossRef]
19. Qas Elias, B.B.; Soh, P.J.; Al-Hadi, A.A.; Akkaraekthalin, P.; Vandenbosch, G.A.E. A Review of Antenna Analysis Using Characteristic Modes. *IEEE Access* **2021**, *9*, 98833–98862. [CrossRef]
20. Balanis, C.A. *Antenna Theory-Analysis and Design*, 2nd ed.; John Wiley and Sons, Inc.: Hoboken, NJ, USA, 1997; ISBN 0-471-59268-4.
21. Bhatnagar, S.K. A New Approach for Designing Rectangular Micro Strip Antenna. In Proceedings of the National Conference on Recent Trends in Microwave Techniques and Applications, Jaipur, India, 30 July–1 August 2012.
22. Mathur, M. Investigations on Design Transformation of Microstrip Antennas and Its Applications in Energy Harvesting. Ph.D. Thesis, Malaviya National Institute of Technology, Jaipur, India, August 2017.
23. Mathur, D.; Bhatnagar, S.K.; Sahula, V. Quick Estimation of Rectangular Patch Antenna Dimensions Based on Equivalent Design Concept. *IEEE Antennas Wirel. Propag. Lett.* **2014**, *13*, 1469–1472. [CrossRef]
24. Guney, K. Simple and Accurate Formulas for the Physical Dimensions of Rectangular Microstrip Antennas with Thin and Thick Substrates. *Microw. Opt. Technol. Lett.* **2005**, *44*, 257–259. [CrossRef]
25. Wang, Z.; Li, X.; Fang, S.; Liu, Y. An Accurate Edge Extension Formula for Calculating Resonant Frequency of Electrically Thin and Thick Rectangular Patch Antennas with and Without Air Gaps. *IEEE Access* **2016**, *4*, 2388–2397. [CrossRef]
26. Kara, M. Formulas for the Computation of the Physical Properties of Rectangular Microstrip Antenna Elements with Various Substrate Thicknesses. *Microw. Opt. Technol. Lett.* **1996**, *12*, 234–239. [CrossRef]
27. Kara, M. Empirical Formulas for the Computation of the Physical Properties of Rectangular Microstrip Antenna Elements with Thick Substrates. *Microw. Opt. Technol. Lett.* **1997**, *14*, 115–121. [CrossRef]

28. Zachou, V.; Mayridis, G.; Christodoulou, C.G.; Chryssomallis, M.T. Transmission Line Model Design Formula for Microstrip Antennas with Slots. In Proceedings of the IEEE Antennas and Propagation Society Symposium, Monterey, CA, USA, 20–25 June 2004; Volume 4, pp. 3613–3616. [CrossRef]
29. Qas Elias, B.B.; Soh, P.J.; Al-Hadi, A.A. A Quick Approximation Method for Estimating the Dimensions of Patch Antennas using CMA. In Proceedings of the 2021 15th International Conference on Advanced Technologies, Systems and Services in Telecommunications (TELSIKS), Nis, Serbia, 20–22 October 2021; pp. 13–16. [CrossRef]